Oxidation State +IV in Group 12 Chemistry. Ab Initio Study of Zinc(IV), Cadmium(IV), and Mercury(IV) Fluorides

Martin Kaupp,*,† Michael Dolg,‡ Hermann Stoll,‡ and Hans Georg von Schnering†

Max-Planck-Institut für Festkörperforschung, Heisenbergstrasse 1, D-70565 Stuttgart, FRG, and Institut für Theoretische Chemie, Universität Stuttgart, Pfaffenwaldring 55, D-70569 Stuttgart, FRG

Received July 8, 1993®

Mercury(IV) fluoride, HgF_4, is thermodynamically stable or only slightly endothermic with respect to gaseous $HgF_2 + F_2$ and might be accessible via fluorination of HgF_2, e.g. by KrF_2. This is the result of high-level quasirelativistic pseudopotential QCISD(T) calculations. In contrast, the existence of CdF_4 is unlikely and that of ZnF_4 even more so. The easier oxidation of HgF_2, compared to CdF_2 or ZnF_2, is due to a relativistic destabilization of the Hg^{II}–F bonds rather than to a relativistic stabilization of HgF_4. Spin–orbit coupling also contributes to a stabilization of HgF_4 vs $HgF_2 + F_2$, but only slightly. The performance of various computational levels to treat electron correlation and of a general basis-set contraction scheme based on atomic natural orbitals have been evaluated. The characterization of molecular HgF_4 should be possible via vibrational spectroscopy, as the calculated harmonic frequencies differ considerably from those of other possible species that might be present in the reaction mixture. Calculations on anionic model complexes and on the dimers $(HgF_4)_2$ and $(HgF_2)_2$ show that HgF_4 gains only limited additional stability by anionic complexation or by aggregation. Thus, any successful synthesis should involve conditions where the lattice energy of HgF_2 is not relevant (e.g. gas-phase molecular beam experiments or reactions in solution).

I. Introduction

The highest known formal oxidation state of the group 12 elements Zn, Cd, and Hg is II.[1-3] Only one single report of a short-lived electrochemically generated Hg(III) species in solution exists.[4] Oxidation of group 12 elements beyond the +II state involves ionization and participation in bonding of the metal $(n-1)$d electrons. This would transform these post-transition metals into transition elements and thus extend the range of the transition metal rows within the periodic table.

Partly due to the relativistic contraction and stabilization of the 6s-orbital and to the relativistic expansion and destabilization of the 5d-orbitals,[5] such an oxidation beyond the +II state is most likely for the heavy element mercury. Table 1 shows the ionization energies (IE) of the group 12 elements. Obviously, the first two IE of mercury are higher, and the third and fourth IE are lower than the corresponding values for Zn or Cd. Inclusion of relativistic effects is essential to reproduce the experimental values for the heavy element mercury. Comparison of the two bottom rows shows the considerable increase of the first and second IE, and the decrease of the third and fourth IE for mercury due to relativity. It is well-known that the +III state is much more important in gold chemistry than for the lighter group 11 elements, Ag and Cu,[1-3] and the largely relativistic origin of this preference for higher oxidation states has been verified.[6] In general, the third-row transition elements tend to exhibit higher oxidation states (or to be more stable in higher oxidation states) than the lighter metals of a given triad.[1-3] Figure 1 shows the trends of the highest known oxidation numbers for the elements of the three transition-metal rows. After a regular increase following the maximum group valency up to Mn(VII), Ru(VIII), and Os(VIII), there is a less regular decrease throughout the last third of a given row. The discovery of Cu(IV) in Cs_2CuF_6[7] and of Au(V) in $CsAuF_5$[8] in the early 1970s has spurred interest in group 12 elements exhibiting valencies above two. However, the above-mentioned report of a short-lived Hg(III) species[4] remains singular.

In analogy to gold(III), we have considered the existence of mercury(IV) by ab initio calculations. In a preliminary communication,[9] we have reported computational evidence that

Table 1. Calculated and Experimental First through Fourth Ionization Energies of the Group 12 Elements (eV)

		I	II	III	IV
Zn	exptl[a]	9.391	17.96	39.7	59.4
	calcd[b]	9.14	17.71	39.64	59.31
Cd	exptl[a]	8.991	16.904	37.47	
	calcd[b]	8.74	16.66	37.42	52.22
Hg	exptl[a]	10.43	18.751	34.2	
	calcd(rel)[b,c]	10.20	18.48	34.17[e]	49.16[e]
	calcd(nr)[b,d]	8.23	15.48	36.01	50.13

[a] Cf. C. E. Moore, *Ionization Potentials and Ionization Limits Derived from the Analysis of Optical Spectra*; National Standard Reference Data Series 34; NBS: Washington, DC, 1970. [b] Averaged coupled pair functional results with ANO-basis (cf. computational methods section). [c] Quasirelativistic ECP. [d] Nonrelativistic ECP. [e] These values include corrections for spin–orbit coupling in $Hg^{3+}(^2D_{5/2})$ (0.77 eV) and in $Hg^{4+}(^3F_4)$ (0.45 eV) obtained in numerical all-electron Dirac–Fock calculations using the program Grasp (Dyall, K. G.; Grant, I. P.; Johnson, C. T.; Parpia, F. A.; Plummer, E. P. *Comput. Phys. Commun.* **1989**, *55*, 425).

* Author to whom correspondence should be addressed. Temporary address from Nov 1993 through Oct 1994: Département de Chimie, Université de Montréal, C.P. 6128, Succ. A, Montréal, Québec H3C 3J7, Canada.
† Max-Planck-Institut für Festkörperforschung.
‡ Universität Stuttgart.
® Abstract published in *Advance ACS Abstracts*, April 1, 1994.

(1) *Comprehensive Coordination Chemistry*; Wilkinson, G., Ed.; Pergamon Press: Oxford, England, 1987; Vol. 5.
(2) Aylett, B. J. In *Comprehensive Inorganic Chemistry*; Trotman-Dickenson, A. F., Ed.; Pergamon Press: Oxford, England, 1973, Vol. 3.
(3) (a) Cotton, F. A.; Wilkinson, G. *Advanced Inorganic Chemistry*, 5th ed.; Wiley: Ed., New York, 1988. (b) Greenwood, N. N.; Earnshaw, A. *Chemistry of the Elements*; Pergamon Press: Oxford, England, 1984.
(4) Deming, R. L.; Allred, A. L.; Dahl, A. R.; Herlinger, A. W.; Kestner, M. O. *J. Am. Chem. Soc.* **1976**, *98*, 4132.
(5) For reviews of relativistic effects on chemical properties, see, e.g.; (a) Pyykkö, P. *Chem. Rev.* **1988**, *88*, 563. (b) Pyykkö, P.; Desclaux, J. P. *Acc. Chem. Res.* **1979**, *12*, 276. (c) Pitzer, K. S. *Acc. Chem. Res.* **1979**, *12*, 271. (d) Schwarz, W. H. E. in *Theoretical Models of Chemical Bonding*; Maksic, B., Ed.; Springer: Berlin, 1990; Vol. 2, p 593.
(6) (a) Schwerdtfeger, P.; Boyd, P. D. W.; Brienne, S.; Burrell, A. K. *Inorg. Chem.* **1991**, *31*, 3481. (b) Schwerdtfeger, P. *J. Am. Chem. Soc.* **1989**, *111*, 7261. (c) Schwerdtfeger, P.; Dolg, M.; Schwarz, W. H. E.; Bowmaker, G. A.; Boyd, P. D. W. *J. Chem. Phys.* **1989**, *91*, 1762. Also see ref 5b.
(7) Harnischmacher, W.; Hoppe, R. *Angew. Chem.* **1973**, *85*, 590; *Angew. Chem.; Int. Ed. Engl.* **1973**, *12*, 582.
(8) Leary, K.; Bartlett, N. *J. Chem. Soc., Chem. Commun.* **1972**, *1*, 903.
(9) Kaupp, M.; v. Schnering, H. G. *Angew. Chem.* **1993**, *105*, 952; *Angew. Chem. Int. Ed. Engl.* **1993**, *32*, 861.

0020-1669/94/1333-2122$04.50/0

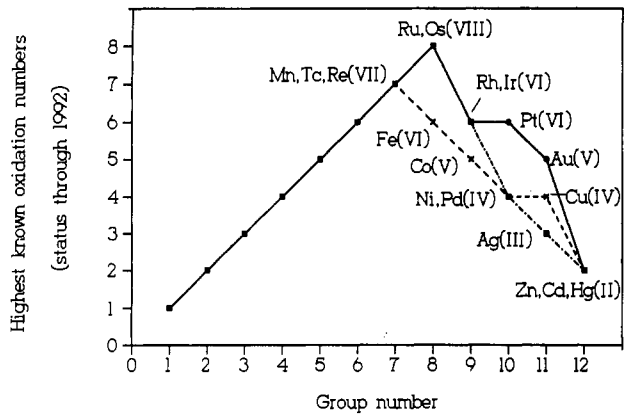

Figure 1. Highest known oxidation numbers for the elements of the first, second, and third transition metal row, respectively.

suggests mercury(IV) fluoride, HgF_4, to have a good chance for existing as a free molecule in the gas phase. A possible preparation route via fluorination of HgF_2 by KrF_2 has been suggested.[9] We now provide a detailed ab initio comparison of the molecular and electronic structures and of the stabilities of HgF_4 and its lighter congeners, ZnF_4 and CdF_4. Different methods to treat electron correlation in these species are evaluated. The influence of relativistic effects on bond distance, stability, and electronic structure of HgF_4 will be discussed. The possible stabilization of HgF_4 by anionic complexation or by aggregation will also be considered.

The setup of this paper is as follows: section II describes the computational methods employed. In section III, we critically compare various theoretical approaches, and establish the accuracy of our calculations. Readers more interested in the general chemical discussion may wish to skip sections II and III. In section IV, the influence of relativistic effects on bond distances and stabilities of HgF_4 and HgF_2 is discussed. In section V, we compare the stability of the tetra- and difluorides of Zn, Cd, and Hg, and discuss possible preparation routes for HgF_4. We detail the electronic structures of the di- and tetrafluorides in section VI. The calculated harmonic vibrational frequencies for HgF_4, HgF_2 and $(HgF_2)_2$ are evaluated in section VII. In section VIII, the possible stabilization of HgF_4 by anionic complexation or by aggregation is discussed. Finally, section IX summarizes our major conclusions.

II. Computational Methods

We have used quasirelativistic 20-valence-electron pseudopotentials for Zn,[10] Cd,[11] and Hg.[11] Comparative calculations with a nonrelativistic Hg pseudopotential[11] provide information on the influence of relativistic effects on molecular properties of the mercury compounds. For Kr and F, we employed quasirelativistic 8- and 7-valence-electron pseudopotentials, respectively.[12,13]

Two different basis-set contraction schemes have been employed: Segmented (8s7p6d)/[6s5p3d] GTO valence basis sets published with the Zn, Cd, and Hg pseudopotentials[10,11] have been used with corresponding segmented valence basis sets for Kr ((6s6p1d)/[4s4p1d])[12] and F ((5s5p1d)/[3s3p1d]).[14] This basis set combination will be designated basis-A. The addition of one metal f-function (cf. Table 2) leads to basis-B. In some cases, a set of two f-functions (Table 2) and a larger (7s7p3d1f)/[5s5p3d1f] fluorine basis[15] have been used (basis-C). To obtain even larger fractions of the electron-correlation energy contributions in post-SCF calculations while keeping the computational effort manageable, we have used a general contraction scheme. Thus, the same primitive metal 8s7p6d2f valence basis sets[10,11] corresponding to basis C have been contracted to 4s3p3d2f using atomic natural orbital (ANO)[16] coefficients obtained in atomic averaged coupled pair functional (ACPF)[17] calculations. Similarly, the Kr 6s6p valence basis[12] was augmented by a 5d3f set[18] and contracted to 2s2p3d2f. The fluorine 7s7p3d1f primitive valence basis set was contracted to a 3s3p3d1f ANO-basis. The ANO contraction coefficients obtained for Zn, Cd, Hg, and F are given in Tables 19–22 in the Appendix. Table 23 in the Appendix shows the atomic ACPF contraction errors with both segmented and general contractions. The performance of segmented vs. general contraction schemes will be discussed in section III.

Table 2. f-Function Exponents Used for Zn, Cd, and Hg[a]

	single f-function	two f-functions
Zn	3.90	6.15, 1.65
Cd	1.80	2.80, 0.80
Hg	0.486	0.95, 0.12

[a] Optimized in atomic QCISD calculations using the quasirelativistic pseudopotentials and segmented 6s5p3d valence bases.

Electron correlation has been included at the second-order Møller-Plesset perturbation theory level (MP2),[19] at the singles + doubles quadratic configuration interaction level (QCISD),[20] and for the most accurate calculations at the QCISD(T) level with perturbation-theoretical inclusion of connected triple substitutions.[20] The ionization energies for Zn, Cd, and Hg given in Table 1 have been calculated at the ACPF level,[17] using the ANO metal basis sets. The calculations employed the Gaussian 90,[21] Gaussian 92,[22] and MOLPRO[23] program systems, except for calculations including spin–orbit coupling, which are described in section IV.

In the following we will use the conventional designations for the computational levels,[24] e.g. a QCISD calculation using basis-B at the structure optimized at the MP2 level using basis-A will be abbreviated by QCISD/basis-B//MP2/basis-A. Full Hartree–Fock (HF) and MP2 geometry optimizations using basis-A have been carried out for MF_4 (M = Zn, Cd, Hg; in D_{4h} symmetry), MF_2 ($D_{\infty h}$), HgF_5^- (in C_{4v} and D_{3h}), HgF_3^- (D_{3h}), HgF_6^{2-} (D_{4h}), HgF_4^{2-} (T_d), $(HgF_2)_2$ (C_{2h}), and $(HgF_4)_2$ (C_{2h}), as well as KrF_2 ($D_{\infty h}$). HF/basis-A harmonic frequency analyses have been performed for all MF_4 and for all mercury species considered (except for $(HgF_4)_2$). The D_{3h} form of HgF_5^- has been found to be a transition state; all other structures are minima at this theoretical level. The M–F distances in MF_4 and in MF_2 have additionally been computed using the MP2/basis-B, the ANO-MP2, and the ANO-QCISD methods.

(10) Dolg, M.; Wedig, U.; Stoll, H.; Preuss, H. *J. Chem. Phys.* **1987**, *86*, 866.
(11) Andrae, D.; Häussermann, U.; Dolg, M.; Stoll, H.; Preuss, H. *Theor. Chim. Acta* **1990**, *77*, 123.
(12) Nicklass, A., Dolg, M.; Stoll, H.; Preuss, H. Unpublished results.
(13) Bergner, A.; Dolg, M.; Küchle, W.; Stoll, H.; Preuss, H. *Mol. Phys.* **1993**, *80*, 1431.
(14) (a) Kaupp, M.; Schleyer, P. v. R.; Stoll, H.; Preuss, H. *J. Am. Chem. Soc.* **1991**, *113*, 6012. (b) *Gaussian Basis Sets for Molecular Calculations*, *Huzinaga*, S., Ed., Elsevier: New York, 1984.
(15) (a) Dolg, M. Dissertation, Universität Stuttgart, 1989. (b) Frisch, M. J.; Pople, J. A.; Binkley, J. S. *J. Chem. Phys.* **1984**, *80*, 3265 (d- and f-exponents, one diffuse sp-set with α = 0.09 has also been added).
(16) Almlöf, J.; Taylor, P. R. *J. Chem. Phys.* **1987**, *86*, 4070.
(17) Gdaniz, R. J.; Ahlrichs, R. *Chem. Phys. Lett.* **1988**, *143*, 413.
(18) The two larger d-exponents of Nicklass' 3d1f polarization set (cf. ref 12), and the three larger d-exponents plus the three f-exponents from the 5d3f set of Maroulis and Thakkar (Maroulis, G.; Thakkar, A. J. *J. Chem. Phys.* **1988**, *92*, 4329) were combined to a 5d3f polarization set for Kr.
(19) Møller, C.; Plesset, M. S. *Phys. Rev.* **1934**, *46*, 618.
(20) See, e.g.; Pople, J. A.; Head-Gordon, M.; Raghavachari, K. *J. Chem. Phys.* **1987**, *87*, 5968. Paldus, J.; Cizek, J.; Jeziorski, B. *J. Chem. Phys.* **1989**, *90*, 4356. **1990**, *93*, 1485. Raghavachari, K.; Head-Gordon, M.; Pople, J. A. *J. Chem. Phys.* **1990**, *93*, 1486.
(21) Frisch, M. J.; Head-Gordon, M.; Trucks, G. W.; Foresman, J. B.; Schlegel, H. B.; Raghavachari, K.; Robb, M.; Binkely, J. S.; Gonzalez, C.; DeFrees, D. J.; Fox, D. J.; Whiteside, R. A.; Seeger, R.; Melius, C. F.; Baker, J.; Kahn, L. R.; Stewart, J. J. P.; Topiol, S.; Pople, J. A. Gaussian 90, Revision F. Gaussian, Inc., Pittsburgh, PA, 1990.
(22) Frisch, M. J.; Trucks, G. W.; Head-Gordon, M.; Gill, P. M. W.; Wong, M. W.; Foresman, J. B.; Johnson, B. G.; Schlegel, H. B.; Robb, M. A.; Replogle, E. S.; Gomperts, R.; Andres, J. L.; Raghavachari, K.; Binkley, J. S.; Gonzalez, C.; Martin, R. L.; Fox, D. I.; DeFrees, D. J.; Baker, J.; Stewart, J. P.; Pople, J. A., Gaussian 92, Revision A. Gaussian, Inc., Pittsburgh, PA, 1992.
(23) Program system MOLPRO written by Werner, H. J.; Knowles, P. J., with contributions by Almlöf, J.; Amos, R.; Elbert, S.; Hampel, C.; Meyer, W.; Peterson, K.; Pitzer, R.; Stone, A.; see, e.g.: (a) Werner, H. J. *Adv. Chem. Phys.* **1987**, *69*, 1. (b) Werner, H. J.; Knowles, P. J. *J. Chem. Phys.* **1988**, *89*, 5803. (c) Knowles, P. J.; Werner, H. J. *Chem. Phys. Lett.* **1988**, *145*, 514 (cf. Hampel, C.; Peterson, K.; Werner, H.-J. *Chem. Phys. Lett.* **1992**, *190*, 1, and references cited therein, for the QCI program).
(24) Explanations of standard levels of theory may be found in: Hehre, W. J.; Radom, L.; Schleyer, P. v. R.; Pople, J. A. *Ab Initio Molecular Orbital Theory*; Wiley: New York, 1986.

Table 3. Comparison of M–F Distances (Å) in MF_4 (M = Zn, Cd, Hg) Calculated at Various Computational Levels (in D_{4h} Symmetry)

M	HF/ basis-A	MP2/ basis A	MP2/ basis-B	ANO-MP2	ANO-QCISD
Zn	1.721	1.827	1.802	1.797	1.736
Cd	1.871	2.010	1.981	1.930	1.872
Hg nr[a]	1.953	2.153	2.050	2.032	1.960
rel[b]	1.886	1.962	1.923	1.904	1.884

[a] Nonrelativistic mercury pseudopotential. [b] Quasirelativistic mercury pseudopotential.

Table 4. Comparison of M–F Distances (Å) in MF_2 (M = Zn, Cd, Hg) Calculated at Various Computational Levels (in $D_{\infty h}$ Symmetry)

M	HF/ basis-A	MP2/ basis-A	MP2/ basis-B	ANO-MP2	ANO-QCISD
Zn	1.743	1.741	1.728	1.717	1.727
Cd	1.949	1.959	1.939	1.908	1.920
Hg nr[a]	2.067	2.079	2.037	2.026	2.036
rel[b]	1.953	1.965	1.924	1.909	1.924

[a] Nonrelativistic mercury pseudopotential. [b] Quasirelativistic mercury pseudopotential.

Reaction energies have been studied at the MP2/basis-B//MP2/basis-A, QCISD/basis-B//MP2/basis-A, and (for some cases) at the ANO-MP2//ANO-MP2, ANO-QCISD//ANO-QCISD, and ANO-QCISD(T)//ANO-QCISD levels. All electrons outside the pseudopotential cores have been correlated in these MP2 and QCI calculations, except for HgF_6^{2-} where, due to program limitations, the 5s and 5p shells on mercury had to be frozen in the QCI calculations (for consistency in the reaction energies, corresponding single-point calculations also have been done for HgF_4^{2-} and HgF_5^-). Calculations of open-shell fragments (e.g. the fluorine atom) are based on UHF reference wave functions.

III. Evaluation of Different Computational Approaches

Bond Distances. Tables 3 and 4 summarize the M–F distances obtained at various theoretical levels for MF_4 and MF_2 (M = Zn, Cd, Hg), respectively. For the tetrafluorides, the HF and the ANO-QCISD results agree within 0.015 Å. The MP2/basis-A distances are considerably too large (by up to 0.1 Å), but the error is slightly reduced upon inclusion of a metal f-function (basis-B). In going from MP2/basis-A to MP2/basis-B to ANO-MP2 (including two metal f-functions), the results approach the ANO-QCISD values. However, the remaining differences r(ANO-MP2) – r(ANO-QCISD) are still ca. 0.06–0.07 Å except for the relativistic Hg-ECP results, where the error is only 0.02 Å. This indicates problems of the MP2 method in describing the bonding in these d^8 species, probably due to nonnegligible nondynamical correlation effects (cf. below). It is tempting to ascribe the bond lengthening from HF/basis-A to MP2/basis-A levels to the influence of "left–right correlation",[25] and the shortening upon inclusion of metal f-functions to angular or core-valence correlation (f-functions are important in describing angular correlation of the $(n-1)$d shell). Interestingly, relativistic effects bring MP2 and QCISD in better agreement for HgF_4. This may indicate reduced nondynamical correlation effects in the quasirelativistic calculations (cf. below).

The agreement between ANO-MP2 and ANO-QCISD distances for the d^{10} difluorides is much better than for the d^8 tetrafluorides, the ANO-MP2 bond lengths being consistently somewhat (ca. 0.01–0.015 Å) shorter. The HF distances are slightly (ca. 0.02–0.03 Å) larger than the ANO-QCISD values. The inclusion of f-functions in the metal basis set (basis-B, ANO) at the correlated level is necessary to reproduce the slight bond shortening compared to the HF values. These results indicate moderate contributions from angular correlation (slightly overestimated by the MP2 method) and considerably reduced left–right correlation compared to the more covalent tetrafluorides.

(25) See, e.g.: Kutzelnigg, W. *Einführung in die Theoretische Chemie: Vol. 2: Die Chemische Bindung*; Verlag Chemie: Weinheim, Germany, 1978.

Table 5. QCISD Valence Energies with Uncontracted Basis Sets,[a] Segmented Basis Sets,[b] and Generally-Contracted ANO Basis-Sets[c] and Contraction Errors

	valence energies, au			errors, 10^{-3} au	
	uncontracted[a]	segmd[b]	ANO[c]	segmd[b]	ANO[c]
Hg	−153.051 415	−152.956 223	−153.035 946	95.2	15.5
F	−24.161 738	−24.154 994	−24.158 058	6.7	3.7
F_2	−48.370 913	−48.357 481	−48.359 738	13.3	11.2
HgF_2	−201.560 472	−201.455 353	−201.527 332	105.1	33.1
HgF_4		−249.805 837	−249.882 323		

[a] 8s7p6d primitive valence basis set for Hg (quasirelativistic ecp); 7s7pd1f for F. [b] Segmented 6s5p3d2f contraction for Hg and 4s4p3d1f for F. [c] ANO 4s3p3d2f contraction for Hg and 3s3p3d1f for F.

Table 6. Effect of Basis Set Contraction[a] on QCISD Reaction Energies (kJ mol^{-1})

reaction	uncontracted	segmd	ANO
$F_2 \rightarrow 2\,F$	124.5	125.0	114.5
$HgF_2 \rightarrow Hg + 2\,F$	487.2	496.6	460.2
$HgF_4 \rightarrow Hg + 4\,F$		602.9	562.2
$HgF_4 \rightarrow HgF_2 + F_2$		−18.6	−12.5

[a] Cf. Table V for basis sets and valence energies.

Basis-Set Contraction Effects on Energies. For an evaluation of the performance of the segmented and ANO general contraction schemes, Table 5 displays the QCISD valence energies for some atoms and molecules, as well as the contraction errors. Table 6 gives various QCISD reaction energies obtained without contraction, with segmented contractions, or with general contractions.

Generally, the absolute contraction errors for the ANO basis sets are smaller than those for the segmented basis sets (cf. Table 5), in spite of the smaller number of contracted groups. While there is not much experience with ANO contractions using pseudopotentials,[26] these results indicate a good performance of the general contraction scheme.

However, as suggested by the atomization energies calculated for F_2, HgF_2, and HgF_4 (Table 6), the atom-optimized ANO basis sets are somewhat biased toward the isolated atoms. Thus, the atomization energies obtained with the ANO basis sets for F_2 and HgF_2 are smaller (by ca. 10–15 kJ mol^{-1} per bond) than the uncontracted-basis results. The values calculated with the segmented basis deviate much less from the atomization energies obtained without basis set contraction, in spite of the smaller electron-correlation energy contributions recovered (note that the SCF contraction errors of the ANO basis sets are larger than those for the segmented contraction). Nevertheless, we will base most of our discussion beyond the MP2 level (QCI, ACPF) on results obtained with the ANO basis sets. The ANO contraction errors in the atomization energies are relatively small, and they tend to cancel, e.g. for the energy of the reaction $HgF_4 \rightarrow HgF_2 + F_2$ (cf. Table 6). Moreover, the smaller number of basis groups involved reduces the computational effort considerably, which is particularly important for the expensive QCISD(T) calculations. For example, a calculation for HgF_4 using the segmented basis-C involves 218 contractions whereas the ANO calculations requires only 178 groups. The corresponding QCI calculation without contraction (268 primitive functions) would in any case be prohibitively expensive.

Performance of MP2, QCISD, and QCISD(T) for Atomization Energies. The atomization energies calculated for MF_2 and MF_4 (M = Zn, Cd, Hg) at the ANO-MP2, ANO-QCISD, and ANO-QCISD(T) levels are shown in Table 7. Taking the best calculations, QCISD(T), as a reference, we note a few general trends:

The performance of MP2 for the difluorides is acceptable, the values consistently being too large (compared to QCISD) by ca.

(26) Sousa, C.; Rubio, J.; Illas, F. *J. Comput. Chem.* **1992**, *13*, 148.

Table 7. Calculated Atomization Energies (kJ mol^{-1}) for MF_4 and MF_2 (M = Zn, Cd, Hg)

	ZPE[a]	ANO-MP2[b]	ANO-QCISD[c]	ANO-QCISD(T)[c]
ZnF_2	−10.2	816.7	736.9	749.1
CdF_2	−8.6	677.7	621.3	636.3
HgF_2 nr[d]	−7.7	680.2	623.0	638.2
rel[e]	−9.2	510.6	460.2	481.2
ZnF_4	−23.2	965.5	593.8	728.4
CdF_4	−22.1	845.7	531.9	679.8
HgF_4 nr[d]	−21.0	861.0	589.5	695.5
rel[e]	−23.4	735.3	562.2	642.7

[a] HF zero-point vibrational energy correction. [b] //ANO-MP2. [c] //ANO-QCISD. [d] Nonrelativistic mercury pseudopotential. [e] Quasirelativistic mercury pseudopotential.

6–9%. The contributions of triple substitutions to the QCI results also are small, 2–4% of the QCISD(T) atomization energies.

For the atomization energies of the tetrafluorides, MP2 performs considerably worse, and the importance of triple excitations is significantly larger: The MP2 values are larger than the QCISD results by up to 33% (for ZnF_4). Relativistic effects for HgF_4 decrease the error from 24% to 14%. The contributions from triple excitations range from ca. 13% (HgF_4, relativistic ECP) to 22% (CdF_4). It is known that contributions from triple substitutions in a single-reference coupled-cluster treatment considerably improve the agreement with multireference CI results in cases with significant but moderate nondynamical correlation contributions, e.g. for F_2, O_3, etc. (also see below).[27] This suggests a larger degree of nondynamical correlation for the tetrafluorides than for the difluorides, which is supported by the weights of the reference determinants in the QCISD calculations (ca. 0.85 for MF_4 but ca. 0.90 for MF_2). Hence, the treatment of electron correlation obviously is more demanding for the tetrafluorides than for the difluorides. We thus expect the ANO-QCISD(T) atomization energies for the latter to be more accurate. Unfortunately, no experimental results are available for the monomeric difluorides.

The failure of MP2 for the binding energies in many transition metal compounds is well documented.[28] The present results allow the performance of MP2 to be compared for compounds of a given central atom (Zn, Cd, or Hg) as a nontransition metal and as a transition metal. Thus, it can easily be verified that the failure of MP2 is intimately connected to the involvement of d-orbitals in bonding. As indicated by the improvement of the performance of MP2 for HgF_4 upon inclusion of the relativistic s-orbital contraction and d-orbital expansion, the problems of a perturbation-theory treatment for the tetrafluorides are also related to a "weak-interaction" situation, i.e. to poor overlap between metal d-orbitals and ligand orbitals. This is consistent with the discussion of electron correlation in closed-shell transition metal compounds given by Buijse and Baerends[29] and with the frequent failure of low orders of the MPn series for systems with appreciably stretched bonds.[30]

Table 8 shows the calculated and experimental atomization energies for KrF_2 and F_2. Similar to the situation for the group 12 tetrafluorides discussed above, the contributions from triple excitations to the atomization energies are considerable for these two species (32% for KrF_2, 20% for F_2), as noted previously for F_2.[27] MP2 overestimates the QCI atomization energies significantly in both cases. The reasonable agreement of the QCISD(T) results with experiment (to within ca. 40 kJ mol^{-1} for KrF_2 and ca. 20 kJ mol^{-1} for F_2), even for the computationally very demanding atomization energy in KrF_2, indicates that the fluorine ANO valence basis-set used is adequate for a good correlation treatment. The agreement with experiment also is important for the discussion of the F_2-elimination reactions (cf. below), and for the possible oxidation of HgF_2 by KrF_2 (cf. section V).

Table 8. Calculated and Experimental Atomization Energies (kJ mol^{-1}) for KrF_2 and F_2

	ZPE[a]	ANO-MP2[b]	ANO-QCISD[c]	ANO-QCISD(T)[c]	exptl
KrF_2	−10.9	+119.4	+21.3	+67.4	+99.5[d]
F_2	−7.1	+166.6	+114.5	+142.9	+154.2[e]

[a] HF zero-point-vibrational energy correction. [b] //ANO-MP2. [c] //ANO-QCISD. [d] Gunn, S. R. *J. Phys. Chem.* **1967**, *71*, 2934. [e] Chase, M. W.; Davies, C. A.; Downey, J. R., Jr.; Frunip, D. J.; McDonald, R. A.; Syverd, A. N. JANAF Thermochemical Tables. *J. Phys. Chem. Ref. Data* **1985**, *14*, Suppl. No. 1.

Table 9. Calculated Reaction Energies (kJ mol^{-1}) for $MF_4 \rightarrow MF_2 + F_2$ (M = Zn, Cd, Hg)

M	ZPE[a]	ANO-MP2[b]	ANO-QCISD[c]	ANO-QCISD(T)[c]
Zn	−5.9	−16.8	−257.6	−163.6
Cd	−6.4	+1.3	−164.5	−99.3
Hg nr[d]	−6.2	+14.2	−148.0	−85.6
rel[e]	−7.1	+63.4	−12.5	+18.7

[a] HF zero-point vibrational energy correction. [b] //ANO-MP2. [c] //ANO-QCISD. [d] Nonrelativistic mercury pseudopotential. [e] Quasirelativistic mercury pseudopotential.

Performance of MP2, QCISD, and QCISD(T) for Energies of F_2-Elimination Reactions. The energies for the reactions $MF_4 \rightarrow MF_2 + F_2$ (M = Zn, Cd, Hg) are shown in Table 9. Due to the much larger errors in the MP2 atomization energies for the tetrafluorides than for the difluorides (cf. above), MP2 strongly overestimates the stability of the former toward F_2-elimination. Again, inclusion of relativistic effects for Hg decreases the discrepancy between MP2 and QCISD(T) (from ca. 100 to ca. 55 kJ mol^{-1}). Similar results have been obtained by Schwerdtfeger et al. for the reaction $AuF_4^- \rightarrow AuF_2^- + F_2$ (quasirelativistic and nonrelativistic ECP MP2, MP3, and MP4 results were compared).[6a]

The contributions from triple excitations to the reaction energies for F_2 elimination range from ca. 31 kJ mol^{-1} (HgF_4 (rel)) to ca. 94 kJ mol^{-1} (ZnF_4). The moderate contributions from triple substitutions for HgF_4 (again reduced by relativistic effects) are responsible for the slight endothermicity obtained for the reaction $HgF_4 \rightarrow HgF_2 + F_2$. Due to smaller nondynamical correlation contributions (cf. above) to the atomization energies for the difluorides than for the tetrafluorides, we expect a better treatment of electron correlation to increase the stability of the tetrafluorides compared to $MF_2 + F_2$. Thus, given a small influence of spin–orbit coupling (cf. section IV), our calculations probably *under*- rather than overestimate the stability of the group 12 tetrafluorides towards F_2 elimination. However, basis-set superposition errors might revert this trend (cf. below).

Influence of Basis-Set Superposition Errors (BSSE) on Stabilities of HgF_4 and HgF_2. To estimate the influence of BSSE on the ANO-QCISD(T) reaction energy for $HgF_4 \rightarrow HgF_2 + F_2$, we have applied the counterpoise correction.[31] Thus, the mercury atom has been calculated in the complete HgF_4 and HgF_2 molecular basis sets. Compared to the atomic basis, the mercury atom is stabilized by ca. 45.1 kJ mol^{-1} in the HgF_4 basis, and by ca. 22.3 kJ mol^{-1} in the HgF_2 basis. Open-shell ANO-QCI calculations of the fluorine atom in the HgF_4 molecular basis have not been possible due to limitations of our computational resources. However, from ANO-MP2 calculations we estimate the counterpoise correction per fluorine atom in HgF_4, HgF_2,

(27) Scuseria, G. E.; Lee, T. J. *J. Chem. Phys.* **1990**, *93*, 5851.
(28) See, e.g.: Marsden, J. C.; Wolynec, P. P. *Inorg. Chem.* **1991**, *30*, 1681. Neuhaus, A.; Frenking, G.; Huber, C.; Gauss, J. *Inorg. Chem.* **1992**, *31*, 5355. Jonas, V.; Frenking, G.; Gauss, J. *Chem. Phys. Lett.* **1992**, *194*, 109.
(29) Buijse, M. A.; Baerends, E. J. *J. Chem. Phys.* **1990**, *93*, 4129.
(30) See, e.g.: Nobes, R. H.; Moncrieff, D.; Wong, M. W.; Radom, L.; Gill, P. M. W.; Pople, J. A. *Chem. Phys. Lett.* **1991**, *182*, 216, and references cited therein.
(31) Boys, S. F.; Bernardi, F. *Mol. Phys.* **1970**, *19*, 553.

Table 10. NPA Metal Net Charge Q, Metal Valence Populations and Relative NAO Contributions to M–F Bonding in MF_4 and MF_2 (M = Zn, Cd, Hg)[a]

		net populations			M–F bonding
	Q	s	p	d	contribns[b]
ZnF_4	2.081	0.335	0.050	9.534	$sp^{0.37}d^{4.76}$
CdF_4	2.201	0.332	0.049	9.418	$sp^{0.14}d^{4.99}$
HgF_4(nr)	2.285	0.295	0.041	9.373	$sp^{0.14}d^{5.62}$
HgF_4(rel)	2.311	0.497	0.053	9.132	$sp^{0.18}d^{6.81}$
ZnF_2	1.756	0.260	0.027	9.957	$sp^{0.06}d^{0.03}$
CdF_2	1.763	0.270	0.024	9.943	$sp^{0.07}d^{0.04}$
HgF_2(nr)	1.803	0.227	0.020	9.946	$sp^{0.07}d^{0.03}$
HgF_2(rel)	1.590	0.568	0.024	9.982	$sp^{0.05}d^{0.13}$

[a] HF/Basis A results. [b] NPA contributions to M–F bonding NLMOs (based on an imposed "no-bond" NBO resonance structure, the metal NAO contributions to the least occupied F lone pair NLMO were analyzed).

and F_2 to be invariably ca. 3.4 kJ mol^{-1} (note that the MP2 and QCISD(T) BSSE estimates for the Hg atom are almost identical). Addition of these combined counterpoise corrections to the ANO-QCISD(T) reaction energy (+18.7 kJ mol^{-1}, cf. Table 9) would lead to a $\Delta E(HgF_4 \rightarrow HgF_2 + F_2)$ of ca. −4.1 kJ mol^{-1}.

IV. The Influence of Relativistic Effects for HgF_4 and HgF_2

Scalar Relativistic Effects on Bond Distances. The two bottom rows in Tables 3 and 4 compare the relativistic and nonrelativistic results for the calculated bond distances in HgF_4 and in HgF_2. As the relativistic effects (i.e. the differences between quasirelativistic and nonrelativistic pseudopotential results) are not the same for different treatments of electron correlation (cf. above), we will concentrate on the best calculations (ANO-QCISD, last columns). While both the bonds in HgF_4 and in HgF_2 are shortened by relativity, the contraction for the former (ca. 0.075 Å) is smaller than that for the latter (ca. 0.112 Å). This is similar to previous results for gold(III) and gold(I) species.[6] Using a simple atomic argument, these differences may be attributed to the different amount of s-orbital involvement in bonding[5,6] (cf. last column in Table 10). While the bonding in the difluorides is dominated by the s-orbitals, the d-orbitals dominate for the tetrafluorides. Thus, for HgF_4 the large relativistic contraction of the 6s-orbital (ca. −0.25 Å for $\Delta_r\langle r\rangle_s$ in $Hg(^1S)$[5c]) is diluted by the moderate relativistic expansion of the 5d-orbitals (weighted average for $\Delta_r\langle r\rangle_d$ in $Hg(^1S)$[5c]: ca. +0.02 Å). The relativistic bond contractions bring the Hg–F distances close to the corresponding Cd–F distances. Note that different interpretations of relativistic effects on bond lengths are possible.[5d,32]

Scalar Relativistic Effects on Stability. In spite of the relativistic bond contraction (cf. above), relativistic effects decrease the atomization energies both for HgF_4 and for HgF_2 (cf. Table 7). However, this relativistic destabilization is significantly larger (ca. 157 kJ mol^{-1}, ca. 25%) for HgF_2 than for HgF_4 (ca. 53 kJ mol^{-1}, ca. 8%). Schwerdtfeger et al. found a relativistic decrease of the atomization energy in AuF (by ca. 60 kJ mol^{-1}), but a relativistic increase for AuF_3 (by ca. 143 kJ mol^{-1}).[6a] However, the latter result is based on Hartree–Fock calculations. Indeed, we obtain a relativistic increase in the atomization energy of HgF_4 (by ca. 122 kJ mol^{-1}) at the HF/basis-B level. This is an artefact due to the better performance of HF (i.e. reduced nondynamical correlation effects, cf. section III) in the quasirelativistic compared to the nonrelativistic ECP regime. To see whether the results of Schwerdtfeger et al. for AuF_3 are also due to the neglect of electron correlation, we have calculated the AuF_3 atomization energy at the nonrelativistic and quasirelativistic MP2/basis-B and QCISD/basis-B levels[33] using the corresponding HF-optimized structures of ref 6a. The quasirelativistic and nonrelativistic QCISD (MP2) results are 582.6 (661.4) and 444.2 (559.3) kJ mol^{-1}, respectively. Thus, as found by Schwerdtfeger et al.,[6a] AuF_3 is indeed stabilized by scalar relativistic effects, in contrast to HgF_4. The better agreement between MP2 and QCISD for AuF_3 compared to HgF_4 also is an interesting result.

These different contributions of relativity to the atomization energies may be rationalized by a simple picture (cf. above for the interpretation of bond length contractions) using the metal s- and d-orbital participation in bonding (cf. Table 10), and bond polarity. In HgF_2 (as in AuF),[6] the relativistically increased 6s-ionization energy leads to a bond destabilization, as the bonding is mainly of the type $Hg^{+2}(F^-)_2$. In HgF_4, this destabilization is diluted by the considerable 5d-orbital contribution to bonding (Table 10). In AuF_3, the relative d-orbital participation in bonding is even larger—hence, the relativistic stabilization. The large relativistic destabilization in HgF_2 due to the relativistically increased 6s-ionization potential of mercury certainly is of general importance for the well-known reluctance[1-3] of Hg(II) to form strong bonds to electronegative elements like fluorine or oxygen.

The differential relativistic stabilization of HgF_4 vs $HgF_2 + F_2$ may be inferred from Table 9. Without relativity, the F_2-elimination reaction would be considerably exothermic, similar to the corresponding reaction for CdF_4. However, this stabilization of oxidation state IV is due to the large relativistic destabilization of HgF_2 and not to a relativistic stabilization of HgF_4 itself! Similar considerations may be important for the discussion of the relative stability of different oxidation states in compounds of other heavy transition metals.

Influence of Spin–Orbit Coupling on Relative Stabilities. To evaluate the importance of spin–orbit (SO) coupling on the stability of HgF_4 vs $HgF_2 + F_2$, we have carried out relativistic 2-component SCF calculations with the program RELMOL.[34] A 20-valence-electron pseudopotential, slightly different from that used throughout the remainder of this study, with a 8s7p6d valence basis for Hg[35] and a 6s6p valence basis for fluorine,[15a] has been employed. The two-component single-point SCF calculations were carried out at the one-component ANO-QCISD optimized geometries (cf. Tables 3 and 4).

The influence of SO coupling is most conveniently discussed as contribution to reaction energies: Spin–orbit coupling stabilizes HgF_4 by ca. 11.1 kJ mol^{-1} with respect to $HgF_2 + F_2$. HgF_2 is further stabilized by ca. 3.9 kJ mol^{-1} vs $Hg + F_2$. Thus, spin–orbit coupling in HgF_4 and in HgF_2 is relatively small and favors the tetrafluoride.

V. The Stability of MF_4 vs. MF_2 (M = Zn, Cd, Hg)

The atomization energies given in Table 7 show that the general order of average M–F bond strength is Zn > Cd > Hg (the relative position of Cd and Hg being due to relativistic effects), *both* in the difluorides *and* in the tetrafluorides. This agrees with the general observation that M–X bond strengths for a given substituent X tend to decrease down group 12.[2] However, the particularly strong bonds in the zinc and cadmium difluorides (QCISD(T) average binding energies are ca. 375 and 318 kJ mol^{-1} in ZnF_2 and CdF_2, respectively) make the existence of the corresponding tetrafluorides extremely unlikely. The QCISD(T) energies for elimination of F_2 from ZnF_4 and CdF_4 are −164 and −99 kJ mol^{-1}, respectively (cf. Table 7), and even the oxidation of gaseous monomeric ZnF_2 by fluorine atoms is calculated to be endothermic by ca. 10 kJ mol^{-1}. Even if the stability of the zinc and cadmium tetrafluorides might come out slightly larger

(32) Schwarz, W. H. E. *Phys. Scr.* **1987**, *36*, 403.
(33) The 19-valence-electron pseudopotentials and (8s7p6d)/[6s5p3d] valence basis sets for Au have been taken from ref 11. A set of f-functions (α = 1.1447) was added (cf. ref 6b).
(34) RELMOL, 2- and 4-component relativistic SCF and MRCI program: Hafner, P.; Esser, M.; Schwarz, W. H. E.; Mark, F.; Schwerdtfeger, P.; Dolg, M., cf. Hafner, P.; Schwarz, W. H. E. *Chem. Phys. Lett.* **1979**, *65*, 357.
(35) Häussermann, U.; Dolg, M.; Stoll, H.; Preuss, H.; Schwerdtfeger, P.; Pitzer, R. M. *Mol. Phys.* **1993**, *78*, 1211.

Table 11. Calculated Reaction Energies (kJ mol^{-1}) for $MF_2 + KrF_2 \rightarrow MF_4 + Kr$

M	ZPE[a]	ANO-MP2[b]	ANO-QCISD[c]	ANO-QCISD(T)[c]
Zn	+2.1	-30.4	+164.4	+88.1
Cd	+2.6	-48.5	+77.2	+23.9
Hg nr[d]	+2.4	-61.4	+54.7	+10.1
rel[e]	+3.3	-111.1	-80.8	-94.2

[a] HF zero-point-vibrational energy correction. [b] //ANO-MP2. [c] //ANO-QCISD. [d] Nonrelativistic mercury pseudopotential. [e] Quasirelativistic mercury pseudopotential.

Table 12. Calculated Harmonic Vibrational Frequencies for HgF_4[a]

symmetry	ω, cm^{-1}	IR active	Raman active
B_{2u}	179	yes	no
A_{2u}	233	yes	no
B_{2g}	252	no	yes
E_u	261	yes	no
B_{1g}	650	no	yes
A_{1g}	652	no	yes
E_u	721	yes	no

[a] HF/basis-A results.

at still higher theoretical levels, the existence of these species is highly improbable.

In contrast, molecular HgF_4 may be stable or only slightly endothermic with respect to $HgF_2 + F_2$, due to the influence of relativistic effects (see above): The best ANO-QCISD(T) calculations (Table 9) corrected for spin–orbit coupling (cf. section IV), zero-point vibrational energy corrections (Table 9), and basis-set superposition errors (cf. section III) yield a reaction enthalpy ($\Delta H°$) of ca. -0.1 kJ mol^{-1}. We estimate that a more complete treatment of electron correlation would yield a slightly positive $\Delta H°$ (cf. section III). Note that lattice energy contributions for HgF_2 will cause a differential stabilization of $HgF_2 + F_2$ vs HgF_4 in the solid state (cf. Section VIII).

Possible Preparation Routes for HgF_4. Krypton difluoride, KrF_2, is a well-known endothermic fluorine compound that has been used as an extremely reactive agent to obtain unusually high oxidation states, e.g. in the preparation of AuF_5.[36] Table 11 shows the reaction energies calculated at various theoretical levels for the oxidation of HgF_2 by KrF_2. For comparison, results for ZnF_2 and CdF_2, as well as nonrelativistic results for HgF_2, are also included.

The discrepancies between the MP2, QCISD, and QCISD(T) atomization energies for the tetrafluorides (cf. Table 7 and section III) are carried over into the energies of the oxidation reactions of ZnF_2, CdF_2, and "nonrelativistic" HgF_2 (cf. Table 11). In all these three cases (top three rows) the best results (ANO-QCISD-(T)) indicate an endothermic reaction, significantly so for Zn. In calculations using the relativistic mercury pseudopotential, the compensation between the MP2 vs. QCISD vs. QCISD(T) differences in the atomization energies of HgF_2, HgF_4, and KrF_2 (cf. Tables 7 and 8) is much better (cf. last row in Table 11), and the different levels agree reasonably well for the oxidation energy. There is little doubt that the reaction $HgF_2 + KrF_2 \rightarrow HgF_4 + Kr$ is significantly exothermic (by ca. 100 kJ mol^{-1}). Thus, the preparation of HgF_4 along this route appears feasable. A major problem is that the reaction has to be carried out under conditions where the lattice energy of HgF_2 is unimportant (cf. discussion in section VIII) but KrF_2 is still stable. This points either to a molecular beam experiment with subsequent mass-spectrometric characterization or matrix isolation of the products or to a low-temperature solvent variant of the reaction. Apparently, there has already been an attempt to conduct the reaction in liquid HF, but no product could be isolated.[37] As the reaction $HgF_2 + 2F \rightarrow HgF_4$ is exothermic by ca. 150 kJ mol^{-1}, one might also speculate about a photochemical reaction involving fluorine atoms. As our calculations indicate that the reaction $HgF_2 + F_2 \rightarrow HgF_4$ may be slightly exothermic (cf. above), even the direct fluorination of HgF_2 under suitable conditions may not be ruled out.

VI. Electronic Structure and Bonding in MF_4 and MF_2 (M = Zn, Cd, Hg)

For an understanding of the different stabilities of ZnF_4, CdF_4, and HgF_4, it is useful to compare the electronic structures of the group 12 di- and tetrafluorides. We have employed the natural population analysis (NPA) and natural bond orbital (NBO) methods.[38] Table 10 gives the metal charges, the metal net *n*s, *n*p, and (*n* - 1)d populations, and an estimate of the relative metal AO contributions to covalent bonding. The latter estimate is based on the analysis of natural atomic orbital (NAO) contributions to natural localized molecular orbitals (NLMO). These in turn have been constructed from a natural bond orbital (NBO) ionic "Lewis structure" ($Hg^{4+} + 4F^-$) with no covalent M–F bonding. The numbers given in the last column of Table 10 thus are the relative contributions from metal s, p, and d orbitals to the resulting least-occupied fluorine lone-pair NLMO (which indeed is M–F σ-bonding). π-Bonding contributions are negligible in all cases.

While the NPA metal charges Q in ZnF_2, CdF_2, and HgF_2 (nonrelativistic calculation) are close to 1.8 (Table 10), relativity reduces this value to ca. 1.6 for HgF_2. This is due to the relativistic increase of the first two ionization energies in mercury (cf. Table 1 and Introduction), which disfavors an ionic configuration, $Hg^{2+}(F^-)_2$, and indeed destabilizes the bonds in HgF_2 appreciably (cf. section IV). The little covalent bonding present in the difluorides is due to the metal s-orbitals (and largely fluorine p-orbitals) with only marginal metal p- or d-orbital participation (a small relativistic increase of the d-contributions is observed for HgF_2; see Table 10).

In contrast to HgF_2, the metal charge in HgF_4 is affected only slightly by relativity and is similar to the charges calculated for ZnF_4 and CdF_4. An increase of the metal charge by only ca. 0.2–0.7 electron (from ca. 1.6–1.8 to ca. 2.2–2.3 electrons) from M(II) to M(IV) indicates significant covalent bonding contributions for the tetrafluorides, as might be expected for a metal in formal oxidation state +IV. However, the distribution of the metal valence population into *n*s, *n*p, and (*n* - 1)d NAOs, and the relative contributions of the metal orbitals to the M–F bonds differ appreciably for the tetrafluorides. The ionization of s-electrons is less pronounced and that of d-electrons is more pronounced for HgF_4 than for its lighter congeners, particularly in the quasirelativistic calculation, HgF_4(rel). Consequently, the d/s ratio of the metal NAO contributions to M–F bonding is larger for HgF_4 (ca. 6.8) than for ZnF_4 and CdF_4 (ca. 4.8–5.0). Comparison with the nonrelativistic HgF_4 results in Table 10 shows that this is to a large extent due to relativity.

The significant d-orbital contributions to bonding indeed characterize the tetrafluorides as genuine transition metal compounds with a formal d^8 configuration, whereas the difluorides (even HgF_2) may be safely regarded as rather ionic d^{10} main group species.

VII. Harmonic Vibrational Frequencies for HgF_4, HgF_2, and $(HgF_2)_2$

Vibrational spectroscopy may be an important method to identify and characterize HgF_4 once obtained. To facilitate the identification, we have performed harmonic vibrational frequency analyses (at the HF/basis-A level) for HgF_4 and HgF_2, and for the HgF_2 dimer. The results are listed in Tables 12–14. The

(36) See, e.g.: Holloway, J. H.; Schrobilgen, G. J. *J. Chem. Soc., Chem. Commun.* **1975**, 78.
(37) Müller, B. Personal communication.
(38) (a) Reed, A. E.; Weinstock, R. B.; Weinhold, F. *J. Chem. Phys.* **1985**, *83*, 735. (b) Reed, A. E.; Weinhold, F. *J. Chem. Phys.* **1985**, *83*, 1736. (c) Reed, A. E.; Curtiss, L. A.; Weinhold, F. *Chem. Rev.* **1988**, *88*, 899.

Table 13. Comparison of Experimental Frequencies and Calculated Harmonic Vibrational Frequencies for HgF_2[a]

symmetry	ω_{calcd}, cm^{-1}	ω_{exptl}, cm^{-1}	IR active	Raman active
Π_u	159	170	yes	no
Σ_g	577	568	no	yes
Σ_u	648	642	yes	no

[a] HF/basis-A results. [b] Given, A.; Loewenschuss, A. *J. Chem. Phys.* **1980**, *72*, 3809.

Table 14. Calculated Harmonic Vibrational Frequencies for $(HgF_2)_2$[a]

symmetry	ω, cm^{-1}	IR active	Raman active
A_u	51	yes	no
A_g	83	no	yes
A_g	86	no	yes
B_u	91	yes	no
B_g	126	no	yes
A_u	168	yes	no
B_u	209	yes	no
A_g	276	no	yes
A_g	479	no	yes
B_u	522	yes	no
B_u	606	yes	no
A_g	611	no	yes

[a] HF/basis-A results.

Table 15. HF Zero-Point Vibrational Energy Corrections (kJ mol^{-1}) for Various Species Considered[a]

species	ZPE	species	ZPE
ZnF_2	10.2	HgF_3^- rel	9.6
CdF_2	8.6	HgF_4^{-2} rel	11.3
HgF_2 nr	7.7	HgF_5^- rel	25.9[b]
rel	9.6	HgF_6^{-2} rel	27.7
ZnF_4	23.2	KrF_2	10.9
CdF_4	22.1	F_2	7.1
HgF_4 nr	20.5		
rel	23.4		

[a] Basis-A results with quasirelativistic (rel) or nonrelativistic (nr) Hg Pseudopotential. [b] In C_{4v} symmetry.

HgF_2 dimer might be one of the species present in a gas-phase molecular beam experiment. Its structure and stability with respect to $2HgF_2$ will be discussed in section VIII. More detailed computational results on this species will be presented elsewhere as part of a study on mercury(II) coordination.[39] The frequencies calculated for HgF_2 are in good agreement with experiment (cf. Table 13). The HF frequencies calculated for AuF_4^- at a basis-set level similar to that used in the present study also agree with experiment to within ca. 10 cm^{-1}.[6a] We expect comparable accuracy for HgF_4.

Due to the high symmetry present, the IR and Raman spectra of HgF_4 can contain no more than 4 and 3 lines, respectively. Moreover, the vibrational wavenumbers of HgF_2 and $(HgF_2)_2$ differ considerably from those of HgF_4 (compare Tables 12–14), particularly in the experimentally most accessible range above ca. 300 cm^{-1}. This should facilitate the identification of HgF_4 by means of vibrational spectroscopy. Results of the harmonic vibrational frequency analyses for HgF_5^-, HgF_6^{-2}, HgF_3^-, HgF_4^{-2}, and KrF_2 are available from the authors upon request. The zero-point vibrational energies calculated for these species, the group 12 di- and tetrafluorides, and F_2 are given in Table 15. They have been employed to calculate the zero-point vibrational energy corrections for the reaction energies given throughout this paper (Tables 7, 8, 11, and 16–18).

VIII. Stabilization of HgF_4 vs HgF_2 by Anionic Complexation or by Aggregation?

Fluoro Complexes: The Model Species HgF_5^-, HgF_6^{2-}, HgF_3^-, and HgF_4^{2-}. Formation of anionic complexes often is a means to stabilize metal species in high oxidation states.[3] Therefore HgF_5^- and HgF_6^{2-} have been considered. For the former, both the trigonal bipyramidal (D_{3h}) and the square pyramidal (C_{4v}) structures have been optimized (Figure 2). At all theoretical levels we find the C_{4v} arrangement to be slightly more stable than the D_{3h} structure (at the HF level, the D_{3h} form is a transition state with one imaginary frequency, whereas the C_{4v} form is a minimum). The best calculated value for the energy difference is ca. 20 kJ mol^{-1} (cf. Table 16). As indicated by the bond lengths,

(39) Kaupp, M.; v. Schnering, H. G. *Inorg. Chem.*, in press.

Table 16. Relative Energies of C_{4v} and D_{3h} Structures for HgF_5^- (kJ mol^{-1})[a]

	ZPE[b]	HF/basis-A	MP2/basis-B	QCISD/basis-B
C_{4v}	25.9	0.0	0.0	0.0
D_{3h}	23.8	+45.6	+10.0	+22.6

[a] Calculated for the MP2/basis-A optimized structures (cf. Figure 2). [b] HF/basis-A zero-point vibrational energy.

Table 17. Calculated Fluoride Attachment Energies (kJ mol^{-1})[a]

reaction	ZPE[b]	HF	MP2	QCISD
$HgF_2 + F^- \rightarrow HgF_3^-$	+0.4	−228.4	−199.1	−208.4
$HgF_3^- + F^- \rightarrow HgF_4^{2-}$	+1.7	+148.5	+167.8	+166.9
$HgF_4 + F^- \rightarrow HgF_5^-$	+2.5	−231.8	−236.8	−234.7
$HgF_5^- + F^- \rightarrow HgF_6^{2-}$	+1.8	+417.9	+364.8[c]	+400.4[c]

[a] Basis-B//MP2/basis-A results. [b] HF zero-point vibrational energy contributions. [c] Mercury 5s and 5p orbitals not correlated.

Table 18. Comparison of QCISD/Basis-B//MP2/Basis-A F_2 Elimination Energies ΔE_f (kJ mol^{-1}) for HgF_4, HgF_5^-, and HgF_6^{2-}

reaction	ΔE_f
$HgF_4 \rightarrow HgF_2 + F_2$	−32.6
$HgF_5^- \rightarrow HgF_3^- + F_2$	−5.9
$HgF_6^{-2} \rightarrow HgF_4^{2-} + F_2$	−249.8[a]

[a] Mercury 5s and 5p orbitals not correlated.

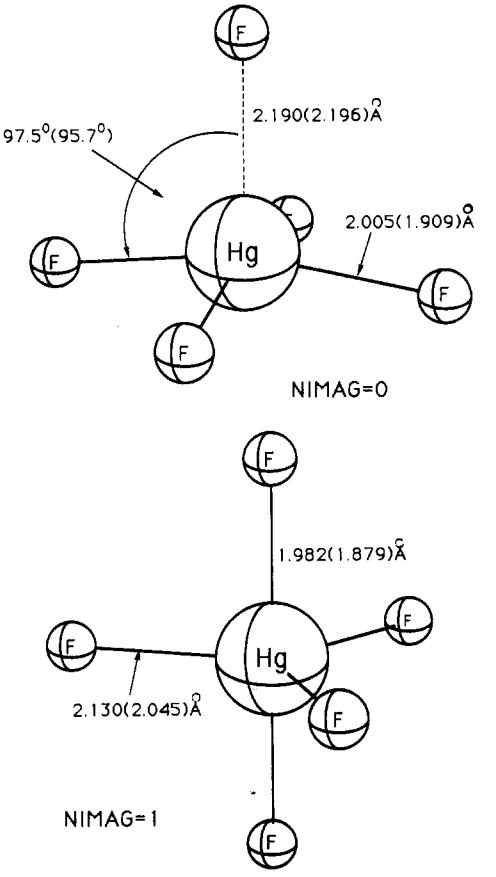

Figure 2. Optimized MP2(HF)/basis-A structures for HgF_5^-: (a, top) C_{4v} structure (minimum); (b, bottom) D_{3h} structure (transition state).

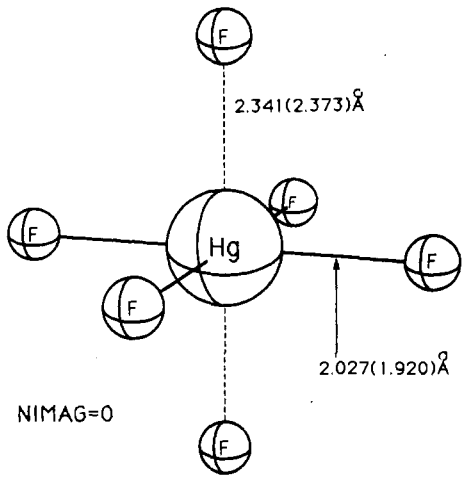

Figure 3. Optimized MP2(HF)/basis-A structures for HgF_6^{2-} in D_{4h} symmetry (HF minimum).

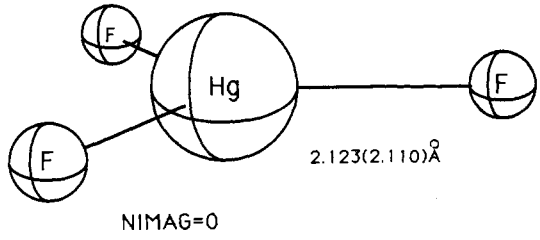

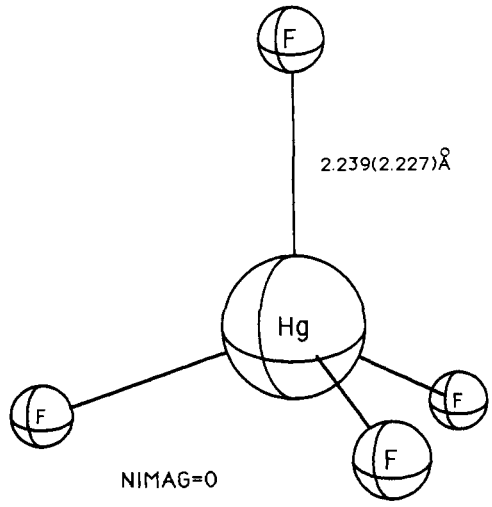

Figure 4. Optimized MP2(HF)/basis-A minimum structures for HgF_3^- and HgF_4^{2-}: (a, top) HgF_3^- in D_{3h} symmetry; (b, bottom) HgF_4^{2-} in T_d symmetry.

the apical secondary Hg–F bond in the C_{4v} structure is considerably less effective than the primary basal bonds (cf. Figure 2). The $F_{ap}HgF_{bas}$ angle is rather close to 90°. Interestingly, the D_{3h} structure exhibits shorter axial than equatorial bonds. As indicated by the rather long secondary bonds in HgF_6^{2-} (Figure 3), binding of a second fluoride ion appears to be still much less effective than that of the first (see below). In contrast, the anionic Hg(II) fluoride complexes HgF_3^- and HgF_4^{2-} feature structures with identical Hg–F bonds (cf. Figure 4), although longer than those in HgF_2 (cf. Table 4). Both the D_{3h} structure for HgF_3^- and the T_d structure for HgF_4^{2-} are minima on their HF/basis-A potential energy surfaces. However, to our knowledge none of these complex anions of mercury(II) fluoride has been observed experimentally.

Table 17 summarizes the QCISD, MP2, and HF results (basis-B) for the energy gained by the attachment of a first and a second fluoride ion to HgF_4 or to HgF_2. While the first fluoride ion is added exothermically, the second addition is endothermic, as

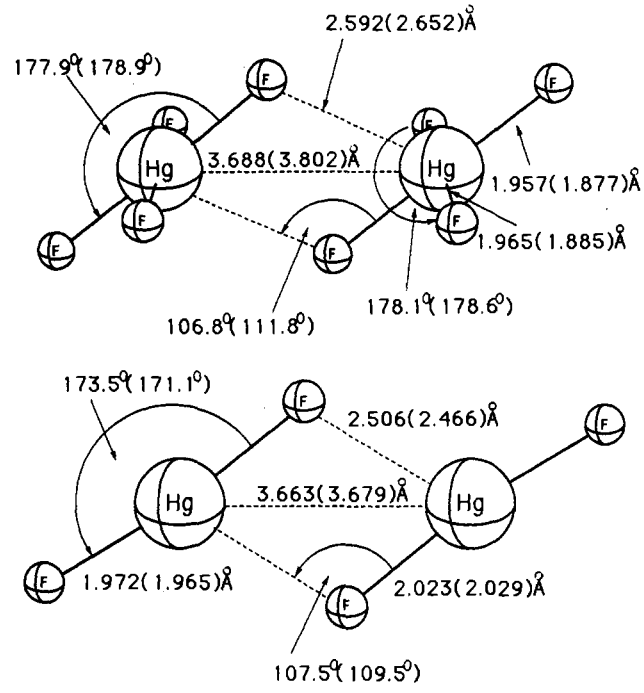

Figure 5. Optimized MP2(HF)/basis-A structures for $(HgF_4)_2$ and $(HgF_2)_2$ in C_{2h} symmetry: (a, top) $(HgF_4)_2$; (b, bottom) $(HgF_2)_2$ (HF minimum).

expected for the free anions. Most importantly, the first addition is slightly more exothermic for HgF_4 than for HgF_2, but the second fluoride addition is far more endothermic for HgF_5^- than for HgF_3^-. Thus, the result suggested by the structures of the anions (Figures 2–4) is borne out by the fluoride attachment energies: The stabilization of Hg(II) by anionic complexation is larger than for Hg(IV). The consequences of the fluoride attachment energies given in Table 17 for the elimination of F_2 from HgF_4, HgF_5^-, or HgF_6^{-2} are shown in Table 18. While F_2-elimination from HgF_5^- is slightly less favorable than for HgF_4 (note the inferior theoretical level compared to the data given in Table 9), addition of a second fluoride ion strongly favors the +II state.

Aggregation: Comparison of $(HgF_4)_2$ and $(HgF_2)_2$. As a first step toward modeling the aggregation of HgF_4 in the condensed phase, in comparison with HgF_2, we have studied the dimers $(HgF_4)_2$ and $(HgF_2)_2$ at the HF/basis-A and MP2/basis-A levels. The optimizations have been carried out in C_{2h} symmetry for both systems, and the results are shown in Figure 5. HF harmonic vibrational frequency analysis (cf. section VII) characterizes the C_{2h} structure as a minimum for $(HgF_2)_2$.

Both dimers represent relatively loose dipole–dipole complexes of the monomers, with only small changes in the monomer structures. However, some differences between $(HgF_4)_2$ and $(HgF_2)_2$ may be noted: In $(HgF_2)_2$ the two secondary bridging Hg···F contacts are shorter (2.506 vs 2.592 Å at the MP2 level), and the lengthening of the primary Hg–F bond involved in bridging (compared to the trans terminal bond) is larger (0.050 vs 0.023 Å). Consequently, the Hg–Hg distance is slightly shorter (3.663 vs 3.688 Å). These structural data for the dimers of HgF_4 and HgF_2 suggest somewhat weaker aggregation for HgF_4, as expected from the smaller Hg–F charge separation (cf. Table 10).

The MP2(HF) dimerization energies for HgF_2 and HgF_4 are 71.6 (79.9) and 66.3 (52.9) kJ mol^{-1}, respectively. Obviously, dimerization of HgF_4 is somewhat less exothermic than that of HgF_2, even though electron correlation favors dimerization of HgF_4 but disfavors that of HgF_2. More importantly, linear HgF_2 has more possibilities of attaching other monomeric units than

(40) Ebert, F.; Woitinek, H. *Z. Allg. Anorg. Chem.* **1933**, *210*, 269.

Table 19. ANO Valence Basis Sets for Mercury 20-Valence-Electron Pseudopotentials[a]

Quasirelativistic Hg Pseudopotential

s-expnt	s-coeff 1	s-coeff 2	s-coeff 3	s-coeff 4
26.842049	−0.016487	−0.005166	0.011839	0.064486
10.320909	0.481214	0.192427	−0.482024	0.006528
6.344923	−1.021718	−0.436569	1.149031	−0.592358
1.450305	0.893341	0.573754	−2.854086	3.335126
0.708215	0.427171	0.256109	2.256339	−4.245811
0.167606	0.038220	−0.729316	0.749619	3.256809
0.059066	0.005940	−0.495895	−1.274802	−2.193251
0.020000	0.001638	0.010126	0.155352	0.320303

p-expnt	p-coeff 1	p-coeff 2	p-coeff 3
9.772990	0.215536	−0.115630	−0.288793
7.169095	−0.447460	0.250436	0.631343
1.868009	0.484007	−0.367818	−1.662077
0.973301	0.532591	−0.442302	0.851331
0.421997	0.161311	0.579243	1.012230
0.125213	−0.000784	0.718047	−0.915838
0.040190	0.001096	−0.010247	−0.065309

d-expnt	d-coeff 1	d-coeff 2	d-coeff 3
4.911447	−0.123758	0.243204	0.654694
3.049550	0.172640	−0.415568	−1.556042
1.344501	0.419545	−0.744942	0.293278
0.576618	0.453967	0.417081	1.025705
0.210245	0.219740	0.603492	−0.873026
0.070000	0.020652	0.060935	−0.118530

Nonrelativistic Hg Pseudopotential

s-expnt	s-coeff 1	s-coeff 2	s-coeff 3	s-coeff 4
20.411181	−0.044460	0.014357	0.027386	0.059987
8.002190	1.303516	−0.453773	−1.208637	0.275483
6.061546	−1.838583	0.656566	1.838931	−0.788059
1.148707	0.990380	−0.504472	−2.812316	2.831256
0.537926	0.346961	−0.238695	2.360890	−3.712767
0.120312	0.021675	0.741711	0.551800	3.270419
0.043510	0.001368	0.470478	−1.154127	−2.435382
0.01500	0.001296	−0.012288	0.155561	0.423676

p-expnt	p-coeff 1	p-coeff 2	p-coeff 3
9.283858	0.189483	−0.081218	0.245753
6.521945	−0.427772	0.190531	−0.579889
1.686345	0.508884	−0.292713	1.527622
0.879019	0.511817	−0.341404	−0.558702
0.393181	0.157464	0.341368	−1.148583
0.112522	0.000328	0.810877	0.690869
0.037595	0.000750	0.073943	0.195725

d-expnt	d-coeff 1	d-coeff 2	d-coeff 3
5.019562	−0.102690	0.204995	0.462876
2.713801	0.188219	−0.469717	−1.485871
1.257831	0.437086	−0.693434	0.567210
0.55344	0.427103	0.537204	0.895729
0.212165	0.186160	0.539035	−0.901531
0.070000	0.014540	0.048959	−0.130511

[a] For pseudopotentials from ref 11.

the planar molecule HgF_4. Indeed, in the solid state HgF_2 adopts the ionic fluorite structure with 8-coordination of mercury.[40] In contrast, the most probable arrangement for HgF_4 is stacking of the square planar d^8 monomers with only two secondary contacts for each mercury atom (leading to a 4 + 2 coordination). A structure of this type has been found for XeF_4.[41] The resulting aggregation energy doubtlessly is much lower than that for HgF_2 (which has a sublimation enthalpy of ca. 120–130 kJ mol^{-1}).[42]

(41) Templeton, D. H.; Zalkin, A.; Forrester, J. D.; Williamson, S. M. *J. Am. Chem. Soc.* **1963**, *85*, 242.

(42) Estimated from heats of formation for solid and gaseous HgF_2 given in: *JANAF Thermochemical Tables*, 2nd ed.; Stull, D. R., Prophet, H., Eds.; Natural Bureau of Standards: Washington, DC, 1971.

Table 20. ANO Valence Basis Set for Quasirelativistic Cadmium 20-Valence-Electron Pseudopotential[a]

s-expnt	s-coeff 1	s-coeff 2	s-coeff 3	s-coeff 4
9.727011	0.967898	−0.347970	−1.176847	3.218841
7.837523	−1.401764	0.520824	1.835648	−5.889629
5.089194	−0.073772	0.009981	−0.095058	2.739625
1.553326	0.852104	−0.407956	−2.430015	1.919264
0.714079	0.443150	−0.285253	1.868638	−3.077957
0.150784	0.030623	0.618139	0.912628	2.835407
0.057467	0.004705	0.548977	−1.266437	−1.924260
0.019000	0.002343	0.021916	0.092126	0.126569

p-expnt	p-coeff 1	p-coeff 2	p-coeff 3
4.742716	−1.049832	0.617143	−2.011322
3.936655	1.110445	−0.703302	2.450079
1.380391	0.624199	−0.300787	0.727893
0.668485	0.233283	−0.185063	−1.344653
0.363423	0.055227	0.569862	−0.212347
0.106253	0.001740	0.680502	0.694924
0.036644	−0.000175	0.017220	0.087590

d-expnt	d-coeff 1	d-coeff 2	d-coeff 3
8.469341	−0.015327	0.050344	−0.079520
3.024231	0.267775	−0.600169	1.154211
1.316367	0.444068	−0.364616	−0.978167
0.556393	0.352313	0.593813	−0.425793
0.223856	0.150063	0.408705	0.821822
0.075000	0.015065	0.053367	0.122709

[a] For Cd pseudopotential from ref 11.

Table 21. ANO Valence Basis Set for Quasirelativistic Zinc 20-Valence-Electron Pseudopotential[a]

s-expnt	s-coeff 1	s-coeff 2	s-coeff 3	s-coeff 4
30.324127	0.090591	−0.023257	−0.171684	0.326101
16.316682	−0.133220	0.037145	0.588268	−1.485539
11.408148	−0.319948	0.083349	−0.092616	1.109691
2.569492	0.730710	−0.248065	−1.894619	1.511895
1.062595	0.478508	−0.242124	1.583970	−2.089971
0.151553	0.022035	0.680726	0.705257	2.129321
0.052747	−0.003885	0.452855	−1.044017	−1.689036
0.010000	0.001489	0.003569	0.080568	0.123022

p-expnt	p-coeff 1	p-coeff 2	p-coeff 3
111.824980	0.002125	−0.000636	−0.003261
19.131910	−0.085188	0.032069	0.141597
5.468838	0.243882	−0.118164	−0.818579
2.505675	0.569141	−0.258713	−0.262107
0.941868	0.317048	0.121553	1.168271
0.171131	0.013626	0.864863	−0.379971
0.049986	−0.002924	0.134839	−0.206282

d-expnt	d-coeff 1	d-coeff 2	d-coeff 3
44.645629	0.041019	0.050970	−0.048688
13.438377	0.187650	0.254468	−0.425250
4.682000	0.388106	0.540314	−0.295173
1.603211	0.439618	−0.189883	1.050903
0.482766	0.283175	−0.654385	−0.583764
0.110000	0.048730	−0.149999	−0.374885

[a] For Zn pseudopotential from ref 10.

IX. Conclusions

Quasirelativistic ab initio pseudopotential calculations, using extended ANO basis sets and high-level methods (QCISD, QCISD(T)) for the treatment of electron correlation, show that mercury tetrafluoride, HgF_4, should exist as a free molecule in the gas phase. The gas-phase reaction $HgF_4 \rightarrow HgF_2 + F_2$ probably is slightly endothermic. In contrast, the existence of CdF_4 and particularly of ZnF_4 is unlikely, as the elimination of F_2 from these metal(IV) fluorides is significantly exothermic. These differences between the lighter group 12 and mercury fluorides are mainly due to the large relativistic destabilization of HgF_2 and not to a direct relativistic stabilization of HgF_4 itself.

Table 22. ANO Valence Basis Set for Quasirelativistic Fluorine 7-Valence-Electron Pseudopotential[a]

s-expnt	s-coeff 1	s-coeff 2	s-coeff 3
57.845327	0.007392	0.006015	0.001029
8.994522	−0.161407	−0.225836	−0.048462
1.578064	0.318474	1.495848	0.385169
0.827850	0.336630	−0.272939	−0.177342
0.413156	0.388629	−0.572064	−0.136198
0.162845	0.094838	−0.610856	−0.036944
0.090	−0.005882	0.106083	0.025648
p-expnt	**p-coeff 1**	**p-coeff 2**	**p-coeff 2**
51.771383	0.012288	0.018142	−0.027959
13.992922	0.070477	0.094751	−0.158059
4.291980	0.221969	0.406090	−0.857131
1.458226	0.408269	0.496918	0.807635
0.473095	0.422363	−0.613845	0.444991
0.129965	0.200644	−0.603147	−1.310470
0.090	−0.053556	0.184486	0.503669

[a] For F pseudopotential from ref 13. To this basis, three d-functions with $\alpha = 3.6, 0.9$, and 0.225 and one f-function with $\alpha = 1.85$ were added.

Possible preparation routes for HgF_4, based on oxidation of HgF_2 by KrF_2, on photochemical oxidation, or on direct thermal fluorination, have been discussed. Computational comparison of the model anions HgF_5^-, HgF_6^{-2}, HgF_3^-, and HgF_4^{2-} indicates that there is no significant stabilization of Hg(IV) vs. Hg(II) by anionic complexation. Similarly, comparison of the dimerization of HgF_4 to that of HgF_2 suggests a larger stabilization of HgF_2 by aggregation. Thus, HgF_4 probably is more volatile than HgF_2, and any preparation route will have to take into account that lattice energy will favor $HgF_2 + F_2$ over HgF_4.

Harmonic vibrational frequencies for HgF_4, HgF_2, and $(HgF_2)_2$ have been calculated to aid the experimental identification of HgF_4. The electronic structures of the group 12 di- and tetrafluorides have been studied by natural population analysis and hybridization analysis. Obviously, the tetrafluorides involve the $(n-1)$d-orbitals in bonding to a significant extent. Thus, they are genuine low-spin d^8 transition metal compounds, whereas the difluorides are true ionic main group (post-transition metal d^{10}) species.

Table 23. Atomic ACPF Contraction Errors (au) for ANO Valence Basis Sets

Hg(rel)[a]	Hg(nr)[b]	Cd	Zn	F
0.015	0.017	0.025	0.046	0.004

[a] With quasirelativistic pseudopotential. [b] With nonrelativistic pseudopotential.

The performance of the MP2 method and the importance of triple substitutions in quadratic CI calculations for the relative energies and structures of the group 12 di- and tetrafluorides have been discussed. Interestingly, for HgF_4 but not for HgF_2 there is a considerable interdependence of relativistic effects (on bond lengths and binding energies) and the level of treatment of electron correlation. This is due to significant nondynamical correlation contributions in HgF_4. These are somewhat smaller in the relativistic than in the nonrelativistic pseudopotential calculations.

Note Added in Proof. The addition of a metal g-function ($\delta = 1.7$) in the ANO-QCISD(T) calculations changes the atomization energies of HgF_4 and HgF_2 by less than 3 kJ mol^{-1} and the reaction energy for $HgF_4 \rightarrow HgF_2 + F_2$ by less than 1 kJ mol^{-1}.

Acknowledgment. We thank Prof. B. Müller (Universität Giessen) for informing us about unpublished attempts to synthesize HgF_4.

Appendix

Tables 19–22 give the atomic-natural-orbital (ANO) valence basis-sets for Hg, Cd, Zn, and F, respectively. The ACPF contraction errors are summarized in Table 23.